Happy hatchday!

How does timing of hatching affect the survival of larval *Gadus morhua* in a changing environment?

Fridtjov Falch Sorø

Master of Science in Biology,
Theoretical Ecology

Department of Biological Sciences
University of Bergen

June 2019

(30 credits)

Acknowledgements

I would like express my gratitude to my supervisors Anders Opdal and Øyvind Fiksen. Thanks for all the constructive feedback you have provided, and for always being available. A special thank you to Anders, for helping me through my cluelessness with regards coding and modelling, and for always having an open office.

A big thank you to all my amazing classmates who have made these times less sufferable, proper #Lektorlove!

To mum and dad, if you ever find the motivation to pick up this piece of work, thanks for, well, being mum and dad! A shout-out to my brothers and sister, and my stepdad as well.

Last, but definitely not least, my sweet girlfriend Amalie! Thanks for being supportive and for encouraging me, and for being the bright light during these dark times (just kidding, writing a master's thesis isn't so bad after all)

Abstract

The classical match-mismatch hypothesis proposes that the timing between larval first feeding and food availability is an important driver of year-class strength. With climate change and the warming of the oceans, it is expected that the spring bloom in temperate waters will start earlier in the year, which may shift the timing of food availability for fish larvae, such as *Calanus finmarchicus* eggs and nauplii. However, decreased water clarity due to climate-driven run-off from terrestrial environments is hypothesised to have the opposite effect, delaying the spring bloom. Here, we present a mechanistic model of the propagation of *C. finmarchicus* eggs and nauplii together with dependent larval *Gadus morhua* growth, and include spring bloom timing, water clarity and visual predation mortality. The results suggest that decreased water clarity reduce visual predation on spawning *Calanus*, leading to increased egg and nauplii food for fish larvae. Increased food availability in addition to the reduced visual predation on cod larvae, may suggest that decreased water clarity increase larval survival at certain optimal spawning times. Due to the responses in larval fitness from decreased water clarity, we suggest that non-chlorophyll light attenuation is an important parameter to consider in future models of fish larvae.

Contents

1. Introduction

There is no lack of attempts to explain the interannual variation in recruitment to a stock of fish (e.g. Litvak and Leggett, 1992, Houde, 1997, Durant et al., 2007). Johan Hjort's (1914) "Critical period" hypothesis was paradigm defining, and became one of the dominant explanations of the recruitment variability for more than 75 years (Houde, 2008). Hjort's critical period referred to the time when a fish larva has exhausted its yolk-sac reserves, and has to shift to external feeding, referred to as first-feeding. First-feeding larva is thought to be highly susceptible to starvation, and changes in planktonic food availability in this period was proposed as one of the most important drivers of variability in year-class strength (Durant et al., 2007). Expanding on Hjort's ideas, Cushing (1990) extended the critical period to cover a longer period of time, the development through larval life and up until metamorphosis, and argued that, in addition to the starvation threat of first-feeding larvae, poorly fed larvae grew more slowly, prolonging the period when they are highly vulnerable to predation. Cushing named his hypothesis the 'match-mismatch hypothesis' (MMH), and emphasized the importance of a temporal match between the peaks in abundance of fish larvae and their planktonic prey for recruitment success (fig. 1) (Cushing, 1990).

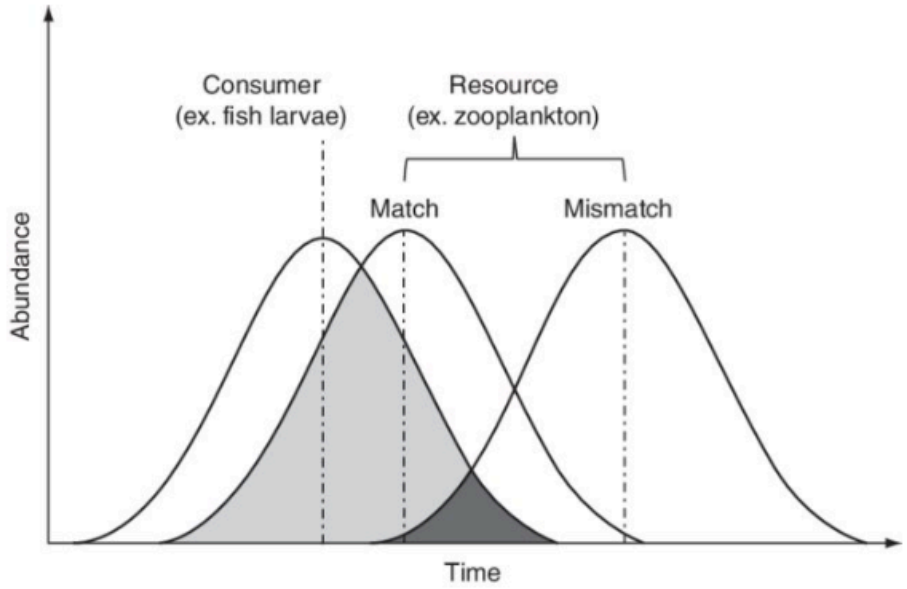

Figure 1: A graphical representation of the match-mismatch hypothesis. The relative overlap between consumer abundance and resources can be a temporal match (light shading), resulting in high consumer population recruitment, or a mismatch (dark shading), with low consumer population recruitment. Reproduced from Kerby et al. (2012)

Empirical support for the MMH has been ambiguous, as it has been difficult to demonstrate it in the field (Leggett and Deblois, 1994). However, it can be argued that this has been the result of data limitations and the simplifications of complex trophic interactions in modelling attempts (Durant et al., 2007). Beaugrand et al. (2003) studied the recruitment variability of Atlantic cod, and suggested a mechanism, involving the MMH, by which variations in temperature affected larval cod survival by bottom-up control, due to rising temperatures changing the plankton ecosystem negatively. Their results supported the MMH, and showed that the survival of larval cod was dependent on three parameters of their prey: their mean size, seasonal timing, and abundance (Beaugrand et al., 2003).

As Cushing (1990) suggested, a temporal match between larval and prey abundances is important, because it is expected that well-fed larvae grows faster and reaches the size where they undergo metamorphosis at a younger age, thus reducing the cumulative mortality rate due to predation during the larval stage, when mortality is known to especially high (Leggett and Deblois, 1994). However, experimental sampling suggests that cod larvae maintains a close-to-maximum growth rate even in circumstances where food availability is low (Folkvord, 2005), due to behavioural changes in the foraging strategy. This is highlighted in modelling efforts of optimal behaviour in larval cod, suggesting that it is difficult to establish a clear relationship between food availability and growth rate (Fiksen and Jørgensen, 2011). Growth rate is predicted to be upheld by a flexible foraging strategy, as low food availability leads to increased risk-taking behaviour. Other modelling efforts produced similar results (Fouzai et al., 2015), that larval growth rate showed little response to prey densities. Growth rate generally increased with temperature, but survival increased with both temperature and prey density (Fouzai et al., 2015). This suggests that food availability is a greater determinant for survival, than for growth rate. A reason for this is that larvae may be motivated to maintain a high feeding rate to support its maximum growth rate, because, while the instantaneous predation risk increases, it lowers the cumulative predator-induced mortality risk during the larval stage (Jørgensen et al., 2014).

One of the most well studied stocks of fish is the Northeast Arctic (NEA) cod stock. It is the commercially most important fish stock of Norway, with an annual export value of around 6 billion NOK (Statistisk Sentralbyrå, 2019). The stock is located in the Barents Sea, with an estimated total stock size of 2.9 million tonnes (2015) (Bakketeig et al., 2017). NEA cod is a

species that performs spawning migrations in the late winter or early spring, leaving their feeding grounds in the Barents Sea, travelling to Coastal Norway to spawn. The most important spawning grounds are located in Lofoten, Norway, but in recent years, a growing number of fish seems to shift their spawning location northwards (Bakketeig et al., 2017). This is not a new phenomenon, as the same pattern was observed in the 1930-1950, but the literature provides no conclusive evidence for the mechanisms behind such changes in spawning locations. For the period 1905 to 1976, Sundby and Nakken (2008) suggested that it might be driven by variations in climate (e.g. higher temperatures) and is possibly caused by a north- and eastward shift in adult distribution on the feeding grounds, that might result in migration routes too far from the southernmost spawning grounds. Combined with higher fecundity and offspring survival due to higher temperature, a larger proportion of the new recruits settles in the northern and eastern parts of the Barents Sea. Contradictory to the results of Sundby and Nakken (2008), statistical analyses by Opdal and Jørgensen (2015) done for an extended time period going back to 1866, produced no significant relationship between spawning ground distribution and climate indicators (i.e. North Atlantic Oscillation index and ocean temperature from the Kola transect), but found that demography had a strong influence on spawning location. This was in line with earlier data (Opdal, 2010) and modelling studies (Opdal, 2010, Jørgensen et al., 2008) pointing towards an effect of fishing on spawning location. While the analysis by Opdal and Jørgensen (2015) suggested no direct effect of neither density dependence nor ocean temperature on spawning locations, a study by Langangen et al. (2019), found otherwise. They found, using a different, more recent dataset (2000-2016), that there was a strong correlation between temperature and spawning latitude.

Additionally, there has been observed a temporal shift in cod phenology, as Pedersen (1984) demonstrated that during 1929-1982, the peak spawning time of NEA cod was delayed by two weeks. Pedersen (1984) argued that a declining mean spawning age due to overexploitation and industrial trawling was the driving force behind the change. This was rooted in the observation that larger and older individuals tended to arrive earlier at the spawning grounds that smaller younger fish. Thus, a reduction in the relative abundance of large fish due to fishing, would shift the median spawning time towards a later date.

Overexploitation of fish stocks have been shown to affects life history traits in a population, as it selects for maturation at an earlier age and smaller size (Olsen et al., 2004). However, the Theoretical Ecology Group of UiB (Opdal, 2018) has scrutinized the same data as Pedersen, and extended the time series back to 1877, before the onset of industrial trawling, and to the present day. During this time series, the pattern is even more pronounced, as peak spawning time has been steadily delayed by about 40 days up until the 1980s, after which it has advanced again. The observation that the delay in spawning time preceded the onset of the industrial trawl fishery in the 1920 (Godø, 2003) may indicate that fisheries-induced changes in demography is not the only driver for the phenological changes in the NEA cod stock, as first suggested by Pedersen (1984). It is also worth noting that such a delay is opposite of what is expected from climate warming, where events in spring are expected to occur earlier in the year, not later (Walther et al., 2002, Poloczanska et al., 2013).

One possible explanation for the observed delay in in spawning could stem from a bottom-up process, starting with the abiotic environment and propagating up through the trophic levels, eventually reaching the spawning cod. A possible starting point, could be the observation of the long-term freshening of Norwegian Coastal waters (1935-2007), in turn resulting in a coastal water darkening (Aksnes et al., 2009) due to increase in e.g. dissolved organic matter (DOM) associated with river run-off (Frigstad et al., 2013). Similar reduction in water clarity has also been observed through shoaling Secchi disk depth in the North Sea and Baltic Sea (Dupont and Aksnes, 2013). Intuitively, darker water increases light attenuation and leads to a shoaling of the euphotic zone, and thus limits the zone of plankton growth and may influence the timing of the phytoplankton bloom (Aksnes, 2015).

Extending this line of reasoning, a shift in phytoplankton bloom may in turn influence the time at which overwintering *Calanus finmarchicus*, an important prey species for larval cod, ascend to the surface to spawn (Heath, 1999), further influencing when Calanus eggs and nauplii are available for first-feeding NEA cod larvae to eat. However, a phytoplankton bloom not only provides feeding opportunities for adult Calanus, but also influences water clarity and thereby predation risk from visual predators – both for Calanus *and* cod larvae. Thus, a decrease in water clarity associated with coastal water darkening (Aksnes et al., 2009) can be expected to influence the feeding efficiency of a visual predator on Calanus and

cod larvae independently of season, while the spring bloom will only influence the visual range in a limited time period.

The seasonal timing of prey availability is highly variable, and the spring peak in plankton production can vary interannually by more than a month (Brander et al., 2001). Due to the consensus that the critical period is important to recruitment success (Cushing, 1990), it is reasonable to assume that the timing of this period is under strong selective pressure. The peak spawning times of cod tend to be just prior to the onset of the spring phytoplankton bloom, and this suggests that the cod is adapted to some average plankton cycle (Brander et al., 2001).

Thus, we have a system with multiple dynamics: (1) coastal darkening reduce water clarity which in turn will affect the visibility for predators *and* fish larvae; (2) coastal darkening may in turn cause a shift in spring bloom timing, changing the seasonal water clarity and the Calanus end date for overwintering, but also the seasonal visibility; (3) because daylight and temperatures are rapidly changing in spring, a shift in bloom timing will influence both zooplankton and larval growth (through temperature) and predation (through day lengths and light levels).

In other words, with so many influencing factors, it is not obvious how this will play out in terms of larval fish survival. Without considering anything else, we expect a late spring bloom, when temperature is high and still increasing rapidly, to lead to higher reproduction rates for Calanus. In turn, this leads to higher prey availability for cod larvae, who will then be able to maintain high growth rates through less effort and increased metabolism, thus increasing their survival. However, as day lengths and light levels increases, how will the potentially intensified predation pressure from fish inhibit the supposedly beneficial consequences of a late bloom for cod larvae, either directly or indirectly through Calanus density control?

To investigate this, we have developed a mechanistic model involving the copepod *C. finmarchicus* and larval cod. We model population dynamics of Calanus in relation to spring bloom timing, visual predation and water clarity, and let individual cod larvae hatch and start feeding in the environment at different times of the year. This enables us to investigate the survival expectancy of cod hatched at different dates, and thus evaluate how the mentioned

environmental factors affect optimal hatching times through the season. In addition, we can also study the effect of a shifting bloom, and try to tear apart the importance of bloom timing in relation to temperature and surface light with regards to optimal time for larval first-feeding. In short, we found that decreased water clarity and a delay in the spring bloom and Calanus production favours late hatchers slightly.

2. Model description

The model description follows the standard protocol for individual-based models recommended by Grimm et al. (2006).

2.1 Purpose

The model was developed to investigate how timing of hatching affects the fitness of larval cod under varying environmental conditions, with a special emphasis on the optical properties of the water. We define larval fitness as the survival probability to 15 mm length. The model follows the propagation of Calanus eggs and nauplii and the successive growth and survival of cod larvae, in relation to spring bloom timing, water clarity, and visual predators. We expect water clarity in Norwegian Coastal waters to decrease due to climate change, and the non-chlorophyll light attenuation coefficient, K_{non}, is an important parameter in this model. Increased K_{non} may have many implications for the trophic interactions along the Norwegian Coast, such as a delayed phytoplankton bloom, changes in abundance and mortality of zooplankton, and reduced foraging efficiency of fish larvae. Thus, the purpose of this modelling effort is to clarify how K_{non} affects the fitness of cod larvae, especially related to timing between hatching date and peaks in prey availability. The simulation occurs at a latitude 68° N, to mimic temperature and light conditions around Lofoten, Norway, which is the historically most important spawning location for NEA cod. The results of this modelling effort might be helpful in furthering our predictive abilities when it comes to fish recruitment in a changing environment.

2.2 State variables and scales

Larval cod are modelled as individuals, with the dynamic state variables age (days), length (m), and weight (mg carbon). Calanus, on the other hand, are structured into different developmental stages, eggs, small nauplii (stage N1-4), large nauplii (stage N5-6), and adult copepods (stage C6). Egg production by adult Calanus females, weigth and the development times for all Calanus stages are temperature-dependent. The habitat is a cubic meter at 20 m depth, characterized by light level (fig. 2A), chlorophyll a concentration and temperature (fig. 2C).

2.3 Process overview and scheduling

Each day of the simulation, the following processes place: larval feeding, growth, mortality, and Calanus egg production, development, and mortality. Larval growth is directly dependent on the feeding rate, which is regulated by light levels in the environment and the presence of appropriately sized prey. Fish larvae that live in an environment without food will expend mass through respiration. Thus, if they do not encounter and catch enough food to compensate for their respiration costs over a prolonged period, their expected survival will be set to zero. Prey is produced by adult Calanus, which are present in the simulation for a limited time, dependent on their seed duration (the period where they enter the simulation) and mortality. Calanus egg production and the development times of the different naupli stages are temperature-dependent, but eggs are produced only after the phytoplankton bloom has started. In this model, temperature is obtained from measurement-station along the Norwegian Coast, extrapolated between the measuring points and idealized to fit the simulation (fig. 2C). The mortality regimes consists of constant daily background mortality rates for Calanus, a size-dependent background mortality rate for fish larvae, and predation-induced mortality for adult Calanus and fish larvae. The predation-induced mortality is regulated by the density of visual predators and their response to the light conditions in the environment.

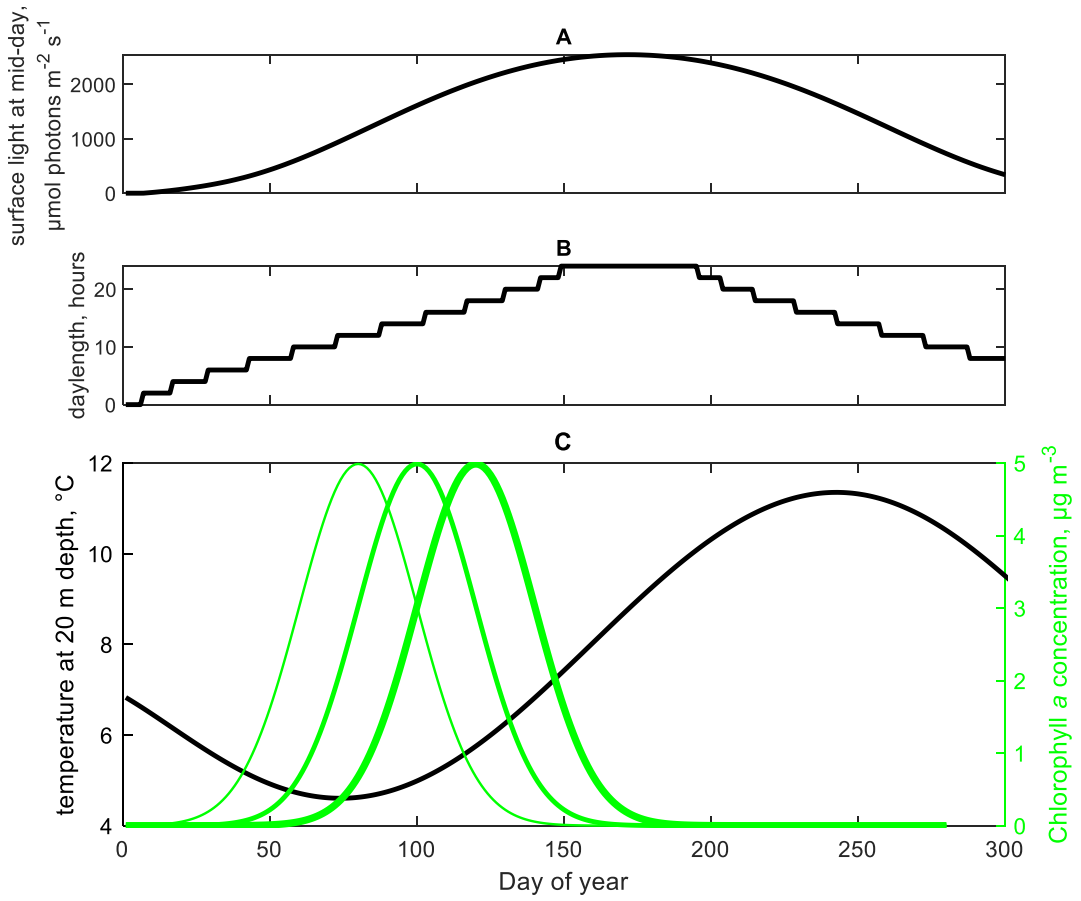

Figure 2: Surface irradiance at mid-day (A), daylengths (B), idealized temperature (C, left x-axis) and chlorophyll a concentration in three different modelling scenarios (C, right x-axis) throughout the simulation periods.

2.3 Initialization

Individual larval cod are introduced in the model at age 1 day with a length of 5 mm, every day from day 1 through day 200. Larvae are modelled to have a maximum age of 80 days, to avoid artificial age bounds, thus the simulation lasts for a total of 280 days. Mature, female Calanus enters in cohorts of 10 individuals per day, from the same day that the phytoplankton bloom starts (fig. 2C), and the following 30 days. The spring phytoplankton bloom is modelled as a normal distribution function, and three scenarios are simulated (fig. 2C). All the initial values are based on data from the literature.

2.4 Submodels

Larval feeding process

As fish larvae are visual foragers (i.e. detects prey by sight), its feeding success is dependent on the rate of which it encounters and detects prey, and its capture success. Detailed models of larval feeding have been developed and applied in earlier modelling efforts (Fiksen and Mackenzie, 2002, Kristiansen et al., 2007, Fiksen and Jørgensen, 2011). Based on those, this model defines larval feeding, *E*, as the mass it ingests per time unit (mg carbon s^{-1}), represented by the equation:

$$E = \frac{C_p \beta_l n_p M_p}{1 + \beta_l n_p} \quad (1)$$

where C_p = 0.2, and represents the prey capture probability of the larvae (Fiksen and Mackenzie, 2002), n_p is the abundance of available prey (# m^{-3}, table 1), M_p is the mean prey carbon weight (mg carbon, *Eq.*14). Larval prey are Calanus eggs and nauplii, whose temperature-dependent carbon weights are the product of functions explained later (subsection "Calanus abundance", eq. 11, 12, 13). The clearance rate, β_l, ($m^3 s^{-1}$), is the parameter that varies with the abiotic environment. It is modelled as:

$$\beta_l = v\pi R^2 u \quad (2)$$

Here, *v* represents the shape of the larva's visual field and is equal to 0.5, due to the assumption that it can only detect prey by looking up or to the sides. The larva's swimming velocity, *u*, are equal to one body length per second.

The visual range, *R* (fig. 4), is a key variable of the clearance rate. It is driven by a complex combination between the physical properties of the environment and physiological and morphological characteristics of both the fish larva and its prey. The prospect of a fish larva spotting a zooplankton prey is dependent on: (i) the prey's body size, also referred to as the image area of the prey (A_p), and its contrast against the background (*z*); (ii) the eye sensitivity, which scales with the relationship between body size and prey size (Fiksen and Mackenzie, 2002); (iii) and the ambient light levels (Aksnes and Utne, 1997) (see table 1 for parameter values). Ambient light levels in the environment of the simulation (20 m depth) is reliant on the level of light attenuation, and the current model distinguishes between light

attenuation from phytoplankton, and attenuation from abiotic factors, such as dissolved organic matter, with the coefficient K_{non} (Woźniak et al., 2003).

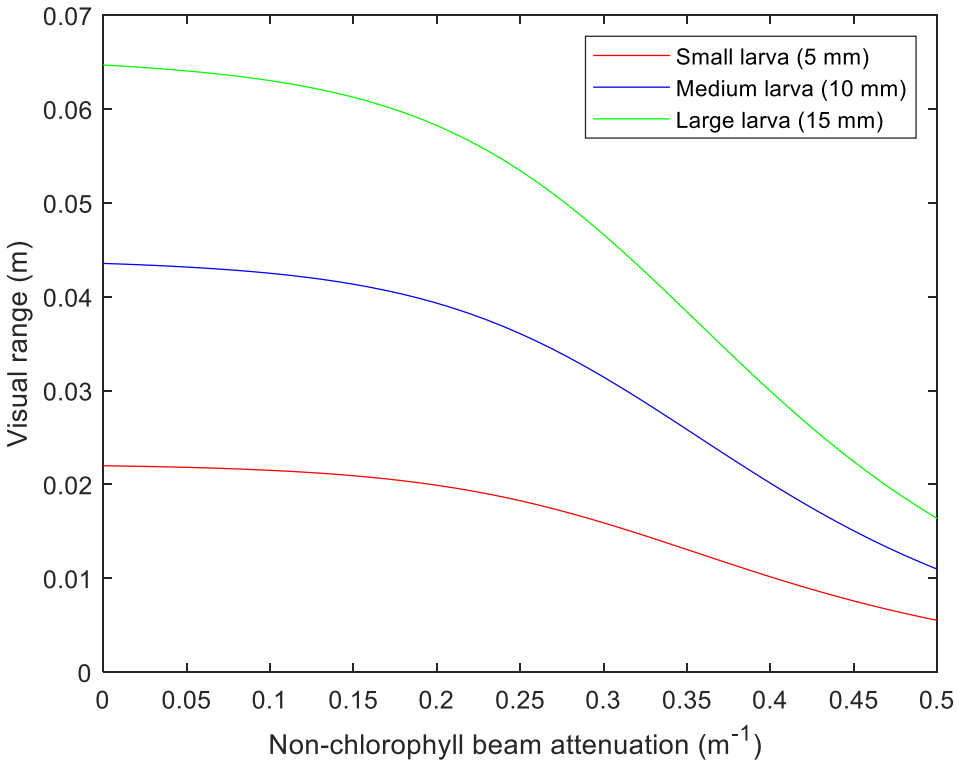

Figure 3: Visual range (m) of cod larvae of small (5 mm), medium (10 mm), and large (15 mm) size, as a function of K_{non}, non-chlorophyll light attenuation. The graphical representation is at midday (h=12) day 100 of the simulation, when chlorophyll concentration is at its peak.

Larval growth rate

Experimental results by Finn et al. (2002) indicated that the respiration rate of larval cod varies with body mass in dry weight, *w* (mg), and temperature, *T* (°C). From Finn et al. (2002), the daily respiration *r* (mg carbon individual^{-1} day^{-1}) is expressed as:

$$r = 2.38 * 10^{-7} w^{0.9} e^{0.088T} s\, dw_c \quad (3)$$

where dw_c is a dry weight-to-carbon conversion constant (table 1), equal to 0.4, as approximately 40% of a larva's dry weight is made up of carbon (Harris et al., 1986). The constant *s* represents seconds in a day, converting the respiration to a daily rate. This

respiration rate is applied in cases where growth is food-limited. Under such conditions, the daily growth rate, *DGR* (mg carbon day^{-1}), is represented by the equation

$$DGR(w,T) = a_f E - dw_c r \quad (4)$$

where a_f is assimilation efficiency, equal to 0.75, to simulate energy losses through behavioural and metabolic processes not related to growth (Kristiansen et al., 2007).

When food is abundant, and the larva is able to capture and ingest more food than it can assimilate, the growth rate is temperature-, and size-limited. Through extensive laboratory experiments, Otterlei et al. (1999) and Folkvord (2005) found the specific growth rate (% day^{-1}) under conditions with an excess of available food to be:

$$SGR(w,T) = a - b\ln(w) - c\ln(w)^2 + d\ln(w)^3 \quad (5)$$

SGR is the specific growth rate in percentage per day, expressed as a function of larval dry weight, *w* (mg), and temperature, *T* (°C) , and *a* = 1.2 + 1.8*T*, *b* = 0.078*T*, *c* = 0.0946*T*, and *d* = 0.0105*T.*

Larval mortality

This model includes the impact of visual predators on the survival of the fish larvae. These predators are typically fish, and their encounter rate with the larvae (m_f, encounters s^{-1}) is expressed as

$$m_f = \beta_f \, d_f \quad (6)$$

where β_f is the clearance rate for a fish predator (m^3 s^{-1}), and d_f the density of fish predators (# m^{-3}). We assume that the fish predators have the same probability of appearing anywhere in the water column, and, since the predators have a higher swimming velocity than the larvae, is able to catch a larva it encounters with certainty. The natural daily mortality of pelagic fish larvae (m_{bg}, day^{-1}) can be expressed as (Mcgurk, 1986):

$$m_{bg} = 2.2x10^{-4}\ (i\ w)^{-0.5} \quad (7)$$

Note that Mcgurk (1986) expression unit is dry weight in *grams*, therefore the conversion of *w* to mg by the constant *i* ($1x10^{-3}$). The product of eq. 7 is multiplied by a factor of 0.5 and added to the product of eq. 6, to give us the daily mortality rate of larval cod, without marginalizing the impact from fish predators.

Calanus abundance

Acting as the food source for larval cod, *C. finmarchicus* are modelled into the environment to replicate and simulate abundances observed in the real environment (Fiksen and Carlotti, 1998). The model does not include any feedback mechanics from the fish larva, i.e. larval feeding does not reduce the number of copepods and nauplii. However, as with the fish larvae, adult Calanus are also susceptible to predation from visual feeders. Their mortality rate from visual feeders ($m_{C6,}$ encounter Calanus^{-1} s^{-1}) are represented as Holling disc-equation parameterized for C6-stage Calanus:

$$m_{C6} = \frac{\beta_f d_f}{1 + \beta_f \Upsilon d_{C6}} \quad (8)$$

where β_f is the encounter rate of the fish predator (table 1), Υ is the handling time of prey (s) by the fish predator (table 1), and d_{C6} is Calanus abundance. This equation yields the mortality rate per second. Eiane et al. (2002) found that observed daily mortality rate in environments dominated by visual feeders tend to be about 0.008 for all developmental stages, but noted that this might be an overestimation with regards to adult copepods. Thus, in this model, a background mortality rate of the adult Calanus equal to 0.035 ($C6_{bg}$, table 1), to account for the dynamic mortality rate from eq. 8.

The fish larvae do not feed on the adult Calanus, but their offspring. Fiksen and Carlotti (1998) created a model of optimal life history in *C. finmarchicus*, and functions for an adult copepod's temperature-dependent reproduction is applied in the current model,

represented as reproduction B_{C6} (number of eggs laid per female, as a function of temperature, *T*):

$$B_{C6} = g\ p_5^T \tag{9}$$

where *g* = 4.8 (scaling factor) and the temperature coefficient p_5 = 1.096 (table 1). Thus, the population dynamics of eggs and nauplii are simple. They are produced by adults, and develops and moults into different naupli stages. The model separates the different pre-mature Calanus stages into two naupliar groups, containing small (N1-N4 stage) and large (N5-N6) nauplii, and a copepodite stage (C1), at which they no longer act as larval prey and leaves the simulation. The development times, *D* (days), between the stages are represented as a function of temperature, retrieved from rearing experiments performed by Campbell et al. (2001):

$$D = \sigma\ (\ T + 9.11\ )^q \tag{10}$$

where σ and *q* are constants (table 1). Each development stage were fit by data matching the time from the midpoint of the egg-laying period to the time where 50% of the copepods had reached a given stage, such that constant σ_{N1} = 595 for the development time from egg to stage NI, and σ_{N5} = 3710 to stage NV. The constant *q* = -2.5. Both eggs and nauplii are modelled to have a daily mortality rate of 0.08, in accordance to findings by Eiane et al. (2002).

Abundance of eggs (n_{egg}), N1-4 (n_{N1}) and N5-6 (n_{N5}) nauplii are retrieved through adult calanus abundance (n_{C6}) and eq. 9 and 10. The weight of Calanus eggs and nauplii are the product of temperature dependent functions from Campbell et al. (2001). For eggs, the weight (mg carbon) is:

$$w_{egg} = \left(h_{egg}\ T + j_{egg}\right)\ i \tag{11}$$

For stages N1-N4 nauplii:

$$w_{N1} = (h_{N1}\ T + j_{N1})\ i \tag{12}$$

For stages N5-N6 nauplii:

$$w_{N5} = (h_{N5}\, T + j_{N5})\, i \tag{13}$$

Note that the products are multiplied with *i* (1x10^{-3}, table) to convert grams to mg. Thus, the mean weight of prey (*Mp*, mg carbon) can be calculated using eq. 11-13 and the egg and nauplii abundances:

$$M_p = \frac{n_{egg}\, w_{egg} + n_{N1}\, w_{N1} + n_{N5}\, w_{N5}}{n_p} \tag{14}$$

where n_p is the total prey abundance (table 1).

Figure 4 illustrates the population dynamics of Calanus in a scenario where the phytoplankton bloom, and thus Calanus introduction, starts at day 40, for three different K_{non} values (0.05; 0.15; 0.3 m^{-1}). With high light attenuation, i.e. K_{non}=0.3 m^{-1}, Calanus survival increases, resulting in greater abundance. Most notably, they remain in the environment longer, prolonging the time when food is available for cod larvae.

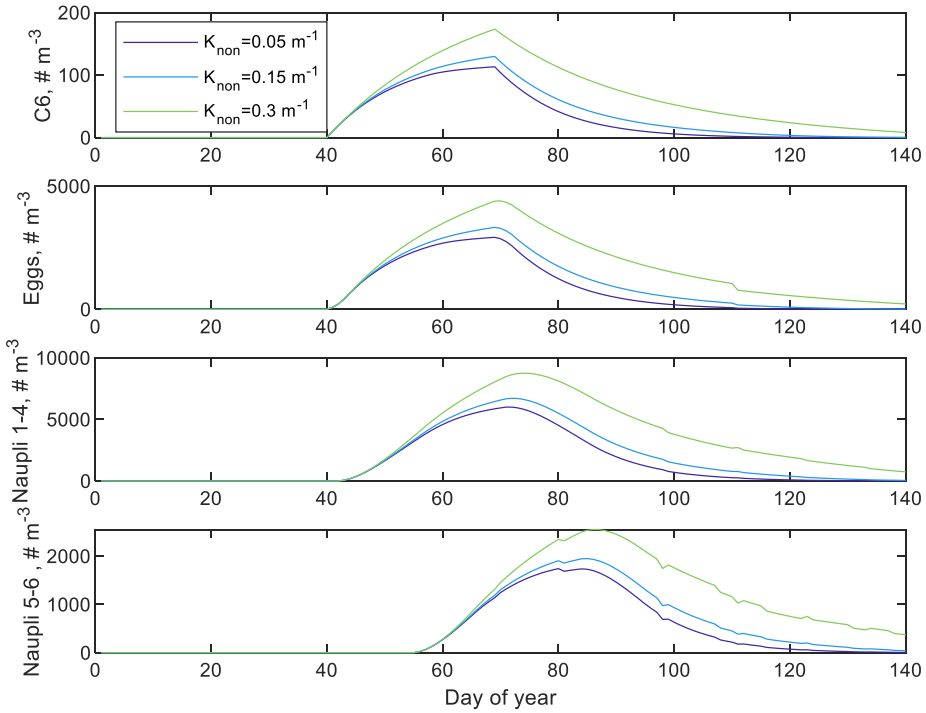

Figure 4: Population dynamics of Calanus under standard conditions, where adult Calanus are introduced at day 40. Colored lines denotes different values of K_{non}, and shows that increased K_{non} leads to higher survival for Calanus.

2.5 Simulation scenarios

We run the model for three scenarios related to the timing of the phytoplankton bloom, and each with three different K_{non} values (0.05; 0.15; 0.3 m^{-1}). The standard scenario is when the bloom starts at day 40 and peaks at day 100. For the two other scenarios, we temporally shift the bloom 20 days in either direction. In all scenarios, Calanus introduction is linked to the start of the phytoplankton bloom. In addition, we also perform a sensitivity analysis by running the same simulation experiments with constant temperature, increased food densities and shallower habitat depth, to investigate whether the same trends as in the regular scenarios unfolds, and how much of an effect these environmental factors have on larval fitness. We did this by manipulating a select variable before running the same scenarios again with: (1) constant seasonal temperature of 4.7° C; (2) a tenfold increase in prey density, by multiplying the egg production rate of Calanus by a factor of 10; (3) a shallower habitat, at 15 meters depth instead of 20 meters.

Table 1: List of parameters, variables, units and values.

Symbol	Variable or parameter	Unit	Value
A_p	Image area of prey	m^{-2}	$1.5x10^{-8}$
a_f	Assimilation efficiency	-	0.75
a	Specific growth rate (*SGR*) parameter	-	1.2 + 1.8*T*
b	Specific growth rate (*SGR*) parameter	-	0.078*T*
β	Clearance rate	$m^3\ s^{-1}$	*Eq.* (2)
B_{C6}	Egg production rate of C6-Calanus	Eggs C6-$Calanus^{-1}$ day^{-1}	*Eq.* (9)
C_p	Prey capture probability of larva	-	0.2
c	Specific growth rate (*SGR*) parameter	-	0.0946*T*
D	Development times for Calanus eggs and nauplii	Day	*Eq.* (10)
DGR	Daily growth rate of fish larva	mg carbon day^{-1}	*Eq.* (4)
d	Specific growth rate (*SGR*) parameter	-	0.0105*T*
d_{C6}	Density of C6-Calanus	# m^{-3}	*"Initialization"*
d_f	Density of fish predator	# m^{-3}	$1.0x10^{-4}$
d_p	Density of food	mg carbon m^{-3}	$n_p * M_p$
dw_c	Conversion constant (dry weight to carbon weight)	mg carbon mg^{-1} dry-$weight^{-1}$	0.4
E	Larval feeding	mg carbon s^{-1}	*Eq.* (1)
g	Scaling factor, Calanus reproduction	-	4.8
h_{egg}	Constant, temperature dependent carbon weight, Calanus egg *(Eq.11)*	-	-0.00255
h_{N1}	Constant, temperature dependent carbon weight, Calanus N1-4 nauplii *(Eq.12)*	-	$9.46x10^{-4}$
h_{N5}	Constant, temperature dependent carbon weight, Calanus N5-6 nauplii *(Eq.13)*	-	-0.0117
j_{egg}	Constant, temperature dependent carbon weight, Calanus egg *(Eq.11)*	-	0.261
j_{N1}	Constant, temperature dependent carbon weight, Calanus N1-4 nauplii *(Eq.12)*	-	0.226
j_{N5}	Constant, temperature dependent carbon weight, Calanus N5-6 nauplii *(Eq.13)*	-	1.825
M_p	Mean weight of prey	mg carbon	*Eq.*(14)

Table 1 (continued)

m_{C6}	C6 mortality rate from fish predators	Encounter Calanus^{-1} s^{-1}	*Eq.* (8)
$C6_{bg}$	C6 background mortality	Day^{-1}	0.035
m_f	Larval mortality from fish predators	Encounter s^{-1}	*Eq.* (6)
m_{bg}	Larval background mortality	Day^{-1}	*Eq.* (7)
n_{egg}	Abundance of Calanus eggs	# m^{-3}	*Eq.(9)(10)*
n_{N1}	Abundance of N1-4 nauplii	# m^{-3}	*Eq.(9)(10)*
n_{N5}	Abundance of N5-6 nauplii	# m^{-3}	*Eq.(9)(10)*
n_p	Total prey abundance	# m^{-3}	$n_{egg} * n_{N1} * n_{N5}$
K_{non}	Non-chlorophyll light attenuation	m^{-1}	0.05; 0.15; 0,3
p_5	Temperature coefficient of Calanus development time	-	1.096
σ_{N1}	Constant, egg development time	-	595
σ_{N5}	Constant, Calanus development time	-	3710
q	Constant, Calanus development time	-	-2.5
R	Visual detection range	m	*Fig*. 4
r	Respiration rate of fish larva	mg carbon ind.$^{-1}$ day^{-1}	*Eq*. (3)
SGR	Specific growth rate of fish larva	% of body weight day^{-1}	*Eq*. (5)
s	Seconds in a day	s day^{-1}	86400
v	Visual field	Proportion of 360°	0.5
u	Swimming velocity	Body length s^{-1}	1
w	Larval dry weight	mg	*Eq.(3)*
w_{egg}	Calanus egg carbon weight	mg carbon	*Eq.*(11)
w_{N1}	Calanus N1-4 naupli carbon weight	mg carbon	*Eq.*(12)
w_{N5}	Calanus N5-6 naupli carbon weight	mg carbon	*Eq.*(13)
γ	Prey handling time	s	2
z	Prey contrast against the background	-	0.3
i	Constant, converting g to mg	-	1x10^{-3}

3. Results

3.1 Optimal hatching times in relation to water clarity and timing of phytoplankton bloom and prey availability

In the first scenario (fig. 5A), when the start of the phytoplankton bloom and the introduction of Calanus was day 20, the optimal hatching times was between day 30 and 60, with the peak date being about 30 days before the peak in prey availability (shaded areas, fig. 5). Such an early bloom favoured larvae living in conditions with intermediate water clarity (K_{non} = 0.15 m^{-1}), as they experienced the highest fitness (maximum recorded fitness = $2.5x10^{-4}$). In the second scenario, where the bloom started at day 40, the optimal hatching times were delayed by about 20 days and narrowed by a small margin (fig. 5B). Still, the larvae in a K_{non} = 0.15 m^{-1} environment experienced highest fitness, but fitness values dropped to about one fifth of what was recorded in the first scenario. A further delay in the phytoplankton bloom (starting day 60, fig. 5C) saw a similar delay of optimal hatching times, but benefited late hatchers in waters with a K_{non} value of 0.3. The results uncovered a trend where, as the phytoplankton bloom and peaks in prey availability was delayed, late hatchers in high K_{non} waters experienced increased fitness. The trend was even more pronounced as the bloom was delayed further.

3.2 Simulation experiments

Temperature

Temperature is rapidly changing through the simulation period (fig. 2C), especially in the period when the phytoplankton bloom starts. To investigate the effect of temperature, we applied a constant seasonal temperature of 4.7° C. The results predicted that larval fitness and optimal hatching times were not sensitive to changes in temperature, as the same pattern appeared (see Appendix A, fig. A1) as in the standard scenarios. This suggests that the seasonal change in temperature (e.g. increased temperature experienced by late hatchers in a late bloom scenario) does not explain the difference in fitness between the scenarios.

Prey density

To test the effect of prey density on larval fitness, we multiplied the egg production rate by adult Calanus by a factor of 10. The fitness patterns remained the same for larvae in waters with a K_{non} value of 0.05. When K_{non} was 0.15, the larvae experienced a slight increase in fitness and the viable hatching window was extended by around 30 days. With K_{non} = 0.3, larval fitness increased greatly, and remained high through all bloom timing experiments, in addition to a large extension on optimal hatching times (a viable hatching window of almost three months). With a late bloom, they experienced more than a tenfold increase in fitness compared to Figure 5C (see Appendix A, fig. A2). As such, food availability seems to be a limiting factor for larval growth in waters with medium to low clarity, as the light conditions may inhibit the foraging efficiency of the larvae.

Habitat depth

When we adjust the habitat depth to 15 meters, it mainly affects the light levels, due to less cumulated beam attenuation through the water masses. A shallower depth led to drastic changes in fitness for the larvae (see Appendix A, fig. A3). Similar to the normal scenarios (fig. 5, left panels), larval fitness in environments with low and medium K_{non}, was predicted to decrease as the bloom was delayed, while recording fitness values much lower than in the normal scenarios. For larvae living in high K_{non}-environments, the same trend with a decrease in fitness as the bloom was delayed, was observed. However, compared to the normal scenarios, they experienced a drastic increase in fitness. In the normal simulations with an early and medium bloom (fig. 5A, B), no larvae in a high K_{non}-environment was expected to either survive or grow to the targeted 15 mm of length. When the habitat was set to 15 m, they reached fitness values of 4.5×10^{-4} (early bloom, optimal hatching day = 40) and 1.2×10^{-4} (medium bloom, optimal hatching day = 60). It is also important to note that this increase in fitness was predicted even though food availability was lower compared to the normal simulations. However, in a late bloom scenario, food density at this depth was so low that the larvae obtained slightly lower fitness than in the scenario plotted in Figure 5C. This, together with the results from the prey density analysis, isolates light conditions as a particularly important variable for larval growth and fitness.

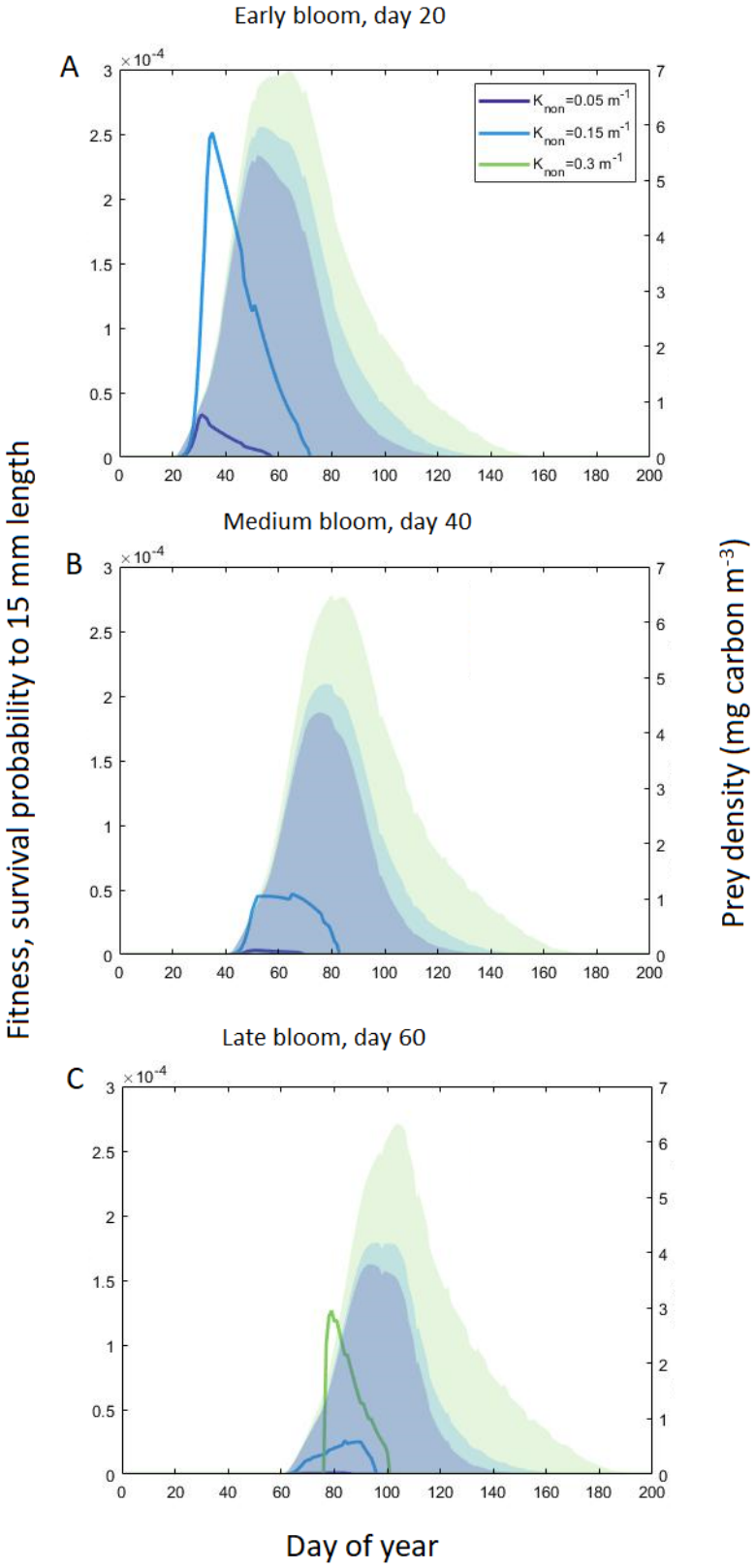

Figure 5: Fitness of hatching times through seasons when the phytoplankton bloom and Calanus production starts at day 20 (A), 40 (B), and 60 (C). Simulations were run for three different K_{non} values (0.05; 0.15; 0.3 m^{-1}). Optimal hatching times are dependent on prey density. When the plankton starts early, larvae living in environments with a K_{non} value of 0.15 m^{-1}(light blue) obtain the highest fitness. A delayed bloom(C) benefits larvae living in conditions with high light attenuation (K_{non}=0.3 m^{-1}, green). Shaded areas represent prey density (mg carbon m^{-3}) for the different K_{non}-scenarios.

4. Discussion

Modelling ecosystem dynamics is a challenging topic, as it is difficult to replicate nature's complex trophic interactions in a simple and precise way. In this study, we tried to tear apart some of the factors we believe affects fish growth and survival, specifically related to the observed delay in spawning times of the NEA cod. To do this, we applied a mechanistic model of the zooplankton *Calanus finmarchicus* population dynamics and the dependent growth and survival of larval cod, in relation to spring bloom timing, water clarity and visual predation mortality. We sought to isolate the environmental factors from each other, to investigate to what extent each of them affects the optimal hatching times of cod through the season. Though *C. finmarchicus* exhibits great asynchrony in the timing of their overwintering wake up (Heath, 1999), we assumed it to be linked to the onset of the spring bloom. We found that as the spring bloom was delayed, the optimal hatching times for cod was delayed as well. A late bloom reduced the fitness (survival probability to 15 mm length) of larvae when light attenuation was low and medium, while it benefited larvae living in waters with high light attenuation. A simulation experiment where we set a constant seasonal temperature did not result in a different fitness pattern, suggesting that the change in larval fitness due to changing bloom timing is not caused by changing temperature (i.e. increasing temperature during a late bloom). However, when manipulating prey densities to become 10 times the normal value, we observed changes in larval fitness in waters with medium and high K_{non}, with larvae in the latter environment experiencing a drastic increase in fitness. Coupled with the results from the experiment where the habitat was set to 15 m, this points to the seasonal light conditions as a very important variable to larval success. It seems to be particulary important with regards to foraging efficiency. This is highlighted by the model result that, in a late bloom scenario with high light attenuation, larval fitness was lower at 15 m depth than at 20 m depth, partly due to lower prey densities. In these scenarios, larval growth rate may be reduced to such a large extent that they never reach the targeted length within a reasonable time period.

All things considered, the model produced a trend that the fitness of hatching times were linked to peaks in prey density, and a delayed bloom favoured larvae in darker waters, compared to waters with a lower K_{non} value. In the introduction, we hypothesized coastal water darkening to play a role in the temporal shift in NEA cod phenology. We proposed a bottom-up mechanism, by which darker waters may lead to a shift in the timing of the spring bloom, in turn changing the timing of when zooplankton end their overwintering slumber. Additionally, the spring bloom affects the level of light attenuation, and combined with darker waters reduces the visibility for predators and fish larvae. Thus, we could expect higher abundances of zooplankton prey for the fish larvae, due to higher temperatures and less predation. While the reduced visibility could be expected to reduce the foraging efficiency of the fish larvae, the combination of increased prey abundance and reduced predation pressure could possibly be beneficial for the survival of the larvae. The model did produce results indicating greater Calanus abundances when light attenuation was high. At the same time, the results suggested that larvae were reliant on quite high food densities to have a realistic chance to survive. The level of non-chlorophyll light attenuation can be highly variable, and the modelled value of 0.3 m^{-1} might be high compared to what we can expect in Norwegian Coastal Waters. Aksnes (2015) developed an empirical model where he, using salinity as a proxy, estimated Norwegian Coastal Water to have an averaged K_{non} value of 0.185 m^{-1}. When we look at the results in scenarios with a K_{non} of 0.15 (fig. 5, light blue), they suggest a trend of decreasing fitness as the phytoplankton bloom is delayed. Thus, there might be some factors that are unaccounted for in our model, making it difficult to evaluate if our hypothesis is supported.

The modelled fitness values for the most viable hatching times fits well within the range predicted by previous models (Fiksen and Jørgensen, 2011, Fouzai et al., 2015), and the size-dependet natural mortality expected for fish larvae (Mcgurk, 1986). However, multiple environmental factors are changing rapidly through the season, especially for the modelled time period. There are few constant variables, and this model proved to be sensitive to changes in prey density and habitat depth. This sensitivity underlines the difficulty in creating a realistic digital environment, as natural fluctuations and interseasonal variations can have a great impact on larval success. Meanwhile, the simplistic nature of the model works well to evaluate the impact specific variables has on larval survival. For instance, the

weak response to changes in water temperature may suggest that the differences in fitness and optimal hatching times between the scenarios cannot be attributed to the seasonal variability in temperature during the duration of the spring bloom. As for Calanus, their development times and egg production rate are temperature-specific, but the model results did not imply an effect of changing temperature on their abundance. In line with the reasoning presented in the introduction, that timing of spawning is under strong selective pressure and linked to peaks in food availability, we can argue that increasing temperature later in the season is not the main driver behind the observed temporal shift in cod phenology.

Modelling behaviour was beyond the scope of this project, but other models have shown that larval survival can be greatly influenced by its behavioural compensations in response to the environment (e.g. Fiksen and Jørgensen, 2011, Fouzai et al., 2015). In the current project, we modelled larvae at a specific depth, but in reality, a larva would migrate vertically, either to shallower, lighter depths and increase its foraging activity, or deeper to avoid visual predators. With increased food availability, optimal behavior will lead to larvae spending less time searching for food at the shallow, well-lit depths, decreasing its probability to be detected and eaten by a visual predator (Fiksen and Jørgensen, 2011). High food availability might also reduce the number daily vertical migrations the larvae has to perform in order to find enough food to sustain a high growth rate, especially for larger larvae (Fouzai et al., 2015). These models predicted that larvae would go to great lengths to maintain a near maximum growth rate because it appeared optimal to accept higher predation than lower growth (Fiksen and Jørgensen, 2011). Thus, the results of these studies suggested a weak link between prey density and growth rate except when food availability is very low, and a strong link between increased survival and increased food and temperature (Fiksen and Jørgensen, 2011). This is somewhat contrary to the results of the current model, as the simulation experiments with increased prey availability implied that slow growth was the inhibiting factor for larvae in water with high light attenuation. Meanwhile, fitness was only recorded for individuals that reached the targeted length, which means that slow growers are eliminated from the results.

The behaviour models of Fiksen and Jørgensen (2011) and Fouzai et al. (2015) did not include a variable non-chlorophyll light attenuation coefficient, K_{non}. By examing the

difference in larval fitness dependent on changes in K_{non}, we might infer the likely behavioural responses of the larvae. For instance, we would expect larvae living in waters with high light attenuation to select shallower habitats than in waters with a lower K_{non}, especially in the case of an early spring bloom. This might illustrate one of the strong points of the model; its usefulness in predicting the outcome of specific situations. Comparing the fitness trends of two scenarios where only one variable is manipulated, might provide valuable predictions that can be accounted for in the development of other ecological models. Aksnes (2015) notes that most ecosystem models does not account for variations non-chlorophyll light attenuation, and calls for an increased attention on it in phytoplankton modelling. As our results indicate, zooplankton abundance and larval fish survival are very responsive changes in light attenuation, and this suggests that K_{non} is an important parameter to include in future models larval behavior and survival.

As for the hypothesis investigated in this thesis, there might be many consequences of coastal water darkening that are not known, and thus not accounted for in the model. Our hypothesis rests on the assumption that there is a link between a darkening of the coastal waters and the *timing* of the spring phytoplankton bloom, but this remains speculative. Additionally, some of the parameters included in this model might not be accurate. For instance, mortality of zooplankton is hard to predict through experimental studies, and their mortality patterns may differ greatly over short distances (Eiane et al., 2002). However, most of the modelled scenarios suggested a slight delay in optimal hatching times relative to the peaks in zooplankton abundance as the phytoplankton bloom was delayed. This might suggest that there is some merit to the hypothesized increased fitness for late hatchers. As larval growth seemed to be sensitive to food densities, by including behavioural mechanisms in models of larvae in environments with high light attenuation, might produce a stronger fitness response. Nevertheless, it proved to be difficult to use such a simple model in evaluating a system with so many dynamic factors. There are several questions that need to be researched before we can draw a conclusion.

5. References

Aksnes, D. L. 2015. Sverdrup critical depth and the role of water clarity in Norwegian Coastal Water. *Ices Journal of Marine Science,* 72**,** 2041-2050.

Aksnes, D. L., Dupont, N., Staby, A., Fiksen, O., Kaartvedt, S. & Aure, J. 2009. Coastal water darkening and implications for mesopelagic regime shifts in Norwegian fjords. *Marine Ecology Progress Series,* 387**,** 39-49.

Aksnes, D. L. & Utne, A. C. W. 1997. A revised model of visual range in fish. *Sarsia,* 82**,** 137-147.

Bakketeig, I. E., Hauge, M. & Kvamme, C. 2017. Havforksningsrapporten 2017. *Fisken og havet.*

Beaugrand, G., Brander, K. M., Lindley, J. A., Souissi, S. & Reid, P. C. 2003. Plankton effect on cod recruitment in the North Sea. *Nature,* 426**,** 661-664.

Brander, K. M., Dickson, R. R. & Shepherd, J. G. 2001. Modelling the timing of plankton production and its effect on recruitment of cod (Gadus morhua). *Ices Journal of Marine Science,* 58**,** 962-966.

Campbell, R. G., Wagner, M. M., Teegarden, G. J., Boudreau, C. A. & Durbin, E. G. 2001. Growth and development rates of the copepod Calanus finmarchicus reared in the laboratory. *Marine Ecology Progress Series,* 221**,** 161-183.

Cushing, D. H. 1990. Plankton Production and Year-Class Strength in Fish Populations - an Update of the Match Mismatch Hypothesis. *Advances in Marine Biology,* 26**,** 249-293.

Dupont, N. & Aksnes, D. L. 2013. Centennial changes in water clarity of the Baltic Sea and the North Sea. *Estuarine Coastal and Shelf Science,* 131**,** 282-289.

Durant, J. M., Hjermann, D. O., Ottersen, G. & Stenseth, N. C. 2007. Climate and the match or mismatch between predator requirements and resource availability. *Climate Research,* 33**,** 271-283.

Eiane, K., Aksnes, D., Ohman, M. D., Wood, S. & Martinussen, M. 2002. Stage-specific mortality of Calanus spp. under different predation regimes. *Limnology and Oceanography,* 47**,** 636-645.

Fiksen, O. & Carlotti, F. 1998. A model of optimal life history and diel vertical migration in Calanus finmarchicus. *Sarsia,* 83**,** 129-147.

Fiksen, Ø. & Jørgensen, C. 2011. Model of optimal behaviour in fish larvae predicts that food availability determines survival, but not growth. *Marine Ecology Progress Series,* 432**,** 207-219.

Fiksen, Ø. & Mackenzie, B. 2002. Process-based models of feeding and prey selection in larval fish. *Marine Ecology Progress Series,* 243**,** 151-164.

Finn, R., Rønnestad, I., Van Der Meeren, T. & J. Fyhn, H. 2002. Fuel and metabolic scaling during the early life stages of Atlantic cod Gadus Morhua. *Marine Ecology Progress Series,* 243**,** 217-234.

Folkvord, A. 2005. Comparison of size-at-age of larval Atlantic cod (Gadus morhua) from different populations based on size- and temperature-dependent growth models. *Canadian Journal of Fisheries and Aquatic Sciences,* 62**,** 1037-1052.

Fouzai, N., Opdal, A. F., Jørgensen, C. & Fiksen, Ø. 2015. Effects of temperature and food availability on larval cod survival: a model for behaviour in vertical gradients. *Marine Ecology Progress Series,* 529**,** 199-212.

Frigstad, H., Andersen, T., Hessen, D., Jeansson, E., Skogen, M., Naustvoll, L., Miles, M., Johannessen, T. & Bellerby, R. 2013. Long-term trends in carbon, nutrients and stoichiometry in Norwegian coastal waters: Evidence of a regime shift. *Prog. Oceanogr.,* 111**,** 113-124.

Godø, O. R. 2003. Fluctuation in stock properties of north-east Arctic cod related to long-term environmental changes. *Fish and Fisheries,* 4**,** 121-137.

Grimm, V., Berger, U., Bastiansen, F., Eliassen, S., Ginot, V., Giske, J., Goss-Custard, J., Grand, T., Heinz, S. K., Huse, G., Huth, A., Jepsen, J. U., Jørgensen, C., Mooij, W. M., Müller, B., Pe'er, G., Piou, C., Railsback, S. F., Robbins, A. M., Robbins, M. M., Rossmanith, E., Rüger, N., Strand, E., Souissi, S., Stillman, R. A., Vabø, R., Visser, U. & Deangelis, D. L. 2006. A standard protocol for describing individual-based and agent-based models. *Ecological Modelling,* 198**,** 115-126.

Harris, R. K., Nishiyama, T. & Paul, A. J. 1986. Carbon, Nitrogen and Caloric Content of Eggs, Larvae, and Juveniles of the Walleye Pollock, Theragra-Chalcogramma. *Journal of Fish Biology,* 29**,** 87-98.

Heath, M. 1999. The ascent migration of Calanus finmarchicus from overwintering depths in the Faroe-Shetland Channel. *Fisheries Oceanography,* 8**,** 84-99.

Hjort, J. 1914. *Fluctuations in the great fisheries of Northern Europe viewed in the light of biological research,* Copenhague, En commission chez Høst.

Houde, E. 2008. Emerging from Hjort's Shadow. *Journal of Northwest Atlantic Fishery Science,* 41**,** 53-70.

Houde, E. D. 1997. Patterns and consequences of selective processes in teleost early life histories. *In:* CHAMBERS, R. C. & TRIPPEL, E. A. (eds.) *Early Life History and Recruitment in Fish Populations.* Dordrecht: Springer Netherlands.

Jørgensen, C., Dunlop, E. S., Opdal, A. F. & Fiksen, Ø. 2008. The evolution of spawning migrations: state dependence and fishing-induced changes. *Ecology,* 89**,** 3436-3448.

Jørgensen, C., Opdal, A. F. & Fiksen, Ø. 2014. Can behavioural ecology unite hypotheses for fish recruitment? *Ices Journal of Marine Science,* 71**,** 909-917.

Kerby, J., Wilmers, C. & Post, E. 2012. Climate change, phenology and the nature of consummer-resource interactions: advancing the match/mismatch hypothesis. *In:* TAKAYUKI OHGUSHI, O. S., ROBERT HOLT (ed.) *Trait-Mediated Indirect Interactions.* Cambridge University Press.

Kristiansen, T., Fiksen, O. & Folkvord, A. 2007. Modelling feeding, growth, and habitat selection in larval Atlantic cod (Gadus morhua): observations and model predictions in a macrocosm environment. *Canadian Journal of Fisheries and Aquatic Sciences,* 64**,** 136-151.

Langangen, O., Farber, L., Stige, L. C., Diekert, F. K., Barth, J. M. I., Matschiner, M., Berg, P. R., Star, B., Stenseth, N. C., Jentoft, S. & Durant, J. M. 2019. Ticket to spawn: Combining economic and genetic data to evaluate the effect of climate and demographic structure on spawning distribution in Atlantic cod. *Global Change Biology,* 25**,** 134-143.

Leggett, W. C. & Deblois, E. 1994. Recruitment in marine fishes: Is it regulated by starvation and predation in the egg and larval stages? *Netherlands Journal of Sea Research,* 32**,** 119-134.

Litvak, M. K. & Leggett, W. C. 1992. Age and size-selective predation on larval fishes: the bigger-is-better hypothesis revisited. *Marine Ecology Progress Series,* 81**,** 13-24.

Mcgurk, M. D. 1986. Natural Mortality of Marine Pelagic Fish Eggs and Larvae - Role of Spatial Patchiness. *Marine Ecology Progress Series,* 34**,** 227-242.

Olsen, E. M., Heino, M., Lilly, G. R., Morgan, M. J., Brattey, J., Ernande, B. & Dieckmann, U. 2004. Maturation trends indicative of rapid evolution preceded the collapse of northern cod. *Nature,* 428**,** 932-935.

Opdal, A. F. 2010. Fisheries change spawning ground distribution in northeast Arctic cod (vol 6, pg 261, 2010). *Biology Letters,* 6**,** 718-718.

Opdal, A. F. 2018. *RE: Anon 1877-2016. Årsberetning vedkommende Norges fiskerier: Lofotfisket (Annual report regarding the Norwegian fisheries: the Lofoten fishery) [In Norwegian] Directorate of Fisheries, Norway.*

Opdal, A. F. & Jørgensen, C. 2015. Long-term change in a behavioural trait: truncated spawning distribution and demography in Northeast Arctic cod. *Global Change Biology,* 21**,** 1521-1530.

Otterlei, E., Nyhammer, G., Folkvord, A. & Stefansson, S. O. 1999. Temperature- and size-dependent growth of larval and early juvenile Atlantic cod (Gadus morhua): a comparative study of Norwegian coastal cod and northeast Arctic cod. *Canadian Journal of Fisheries and Aquatic Sciences,* 56**,** 2099-2111.

Pedersen, T. 1984. Variation of peak spawning of Arcto-Norwegian cod (Gadus morhua L.) during the time period 1929-1982 based on indices estimated from fishery statistics. *In:* DAHL, E., DANIELSSEN, D.S., MOSKNESS, E., SOLEMDAL, P. (ed.) *The propagation of cod (Gadus morhua L.). Flødevigens rapportserie 1.* Arendal, Norway.

Poloczanska, E. S., Brown, C. J., Sydeman, W. J., Kiessling, W., Schoeman, D. S., Moore, P. J., Brander, K., Bruno, J. F., Buckley, L. B., Burrows, M. T., Duarte, C. M., Halpern, B. S., Holding, J., Kappel, C. V., O'connor, M. I., Pandolfi, J. M., Parmesan, C., Schwing, F., Thompson, S. A. & Richardson, A. J. 2013. Global imprint of climate change on marine life. *Nature Climate Change,* 3**,** 919-925.

Statistisk Sentralbyrå. 2019. *Fiskeri* [Online]. Available: https://www.ssb.no/jord-skog-jakt-og-fiskeri/statistikker/fiskeri [Accessed 25.05 2019].

Sundby, S. & Nakken, O. 2008. Spatial shifts in spawning habitats of Arcto-Norwegian cod related to multidecadal climate oscillations and climate change. *ICES Journal of Marine Science,* 65**,** 953-962.

Walther, G. R., Post, E., Convey, P., Menzel, A., Parmesan, C., Beebee, T. J. C., Fromentin, J. M., Hoegh-Guldberg, O. & Bairlein, F. 2002. Ecological responses to recent climate change. *Nature,* 416**,** 389-395.

Woźniak, B., Jerzy, D., Ficek, D., Majchrowski, R., Mirosława, O. & Kaczmarek, S. 2003. Modelling light and photosynthesis in the marine environment. *Oceanologia,* 45.

Appendix A – Figures of simulation experiments (3.2)

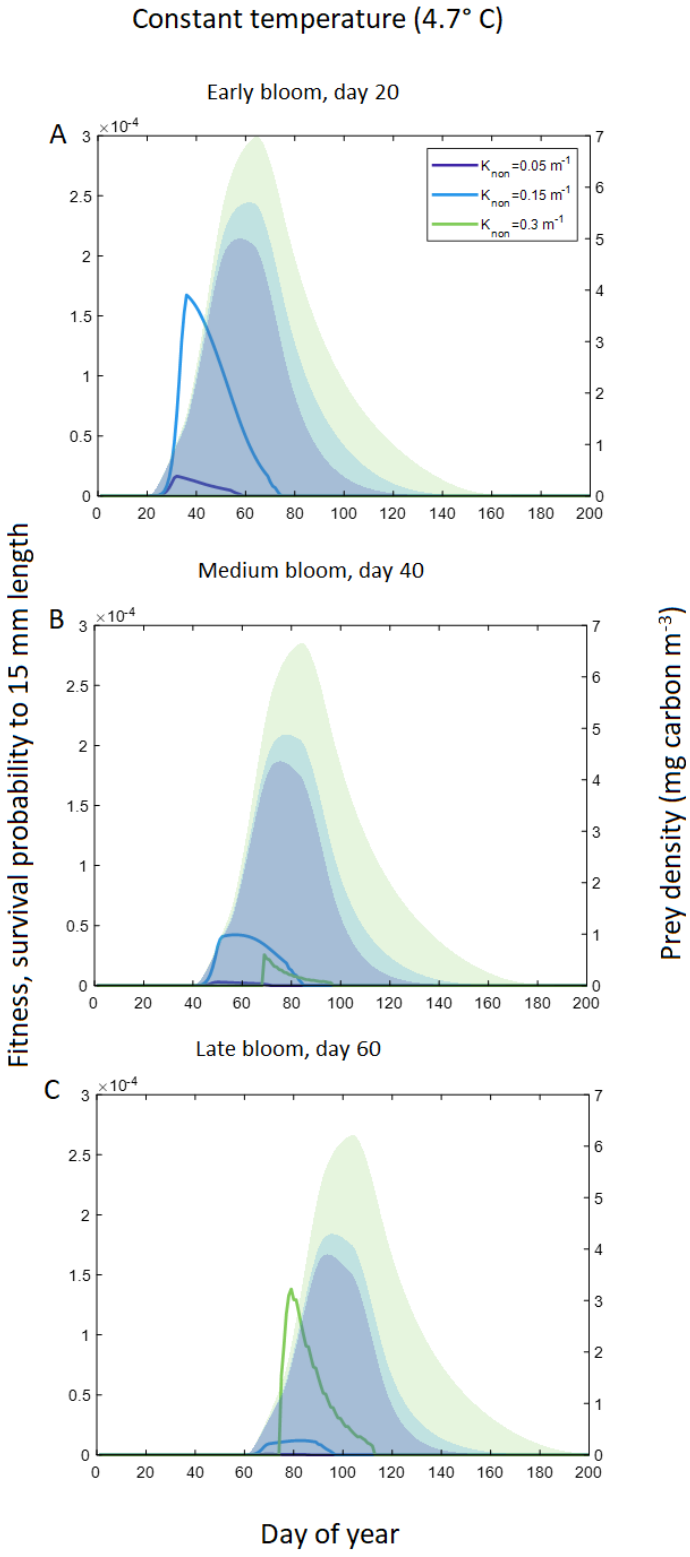

Figure A1: Simulation experiment with a constant seasonal temperature, 4.7° C. Fitness of hatching times through seasons when the phytoplankton bloom and Calanus production starts at day 20 (A), 40 (B), and 60 (C). Simulations were run for three different K_{non} values (0.05; 0.15; 0.3 m^{-1}). Shaded areas represents prey density, each colour corresponding to a different K_{non}. The pattern is similar to the results of Figure 5.

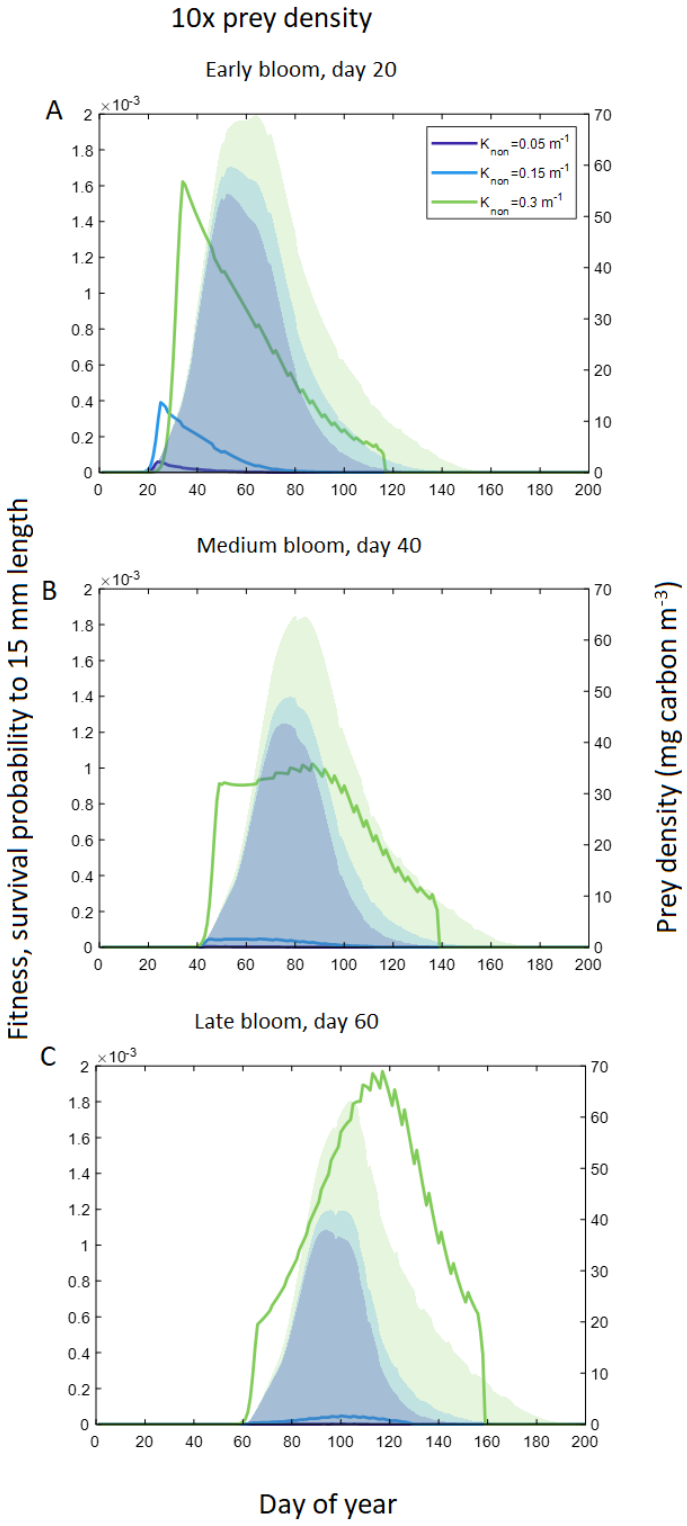

Figure A2: Simulation experiment where Calanus egg production rate was increased by a factor of 10. The panels represents scenarios where the phytoplankton bloom and Calanus production starts at day 20 (A), 40 (B), and 60 (C). Simulations were run for three different K_{non} values (0.05; 0.15; 0.3 m^{-1}). Shaded areas represents prey density, each colour corresponding to a different K_{non}..With high light attenuation (Knon=0.3 m-1, green), viable spawning windows broadened widely compared to the normal scenarios (fig. 5). The viable spawning window broadened with medium light attenuation as well, but resulted in lower fitness of the hatching times than in the normal scenarios (fig. 5).

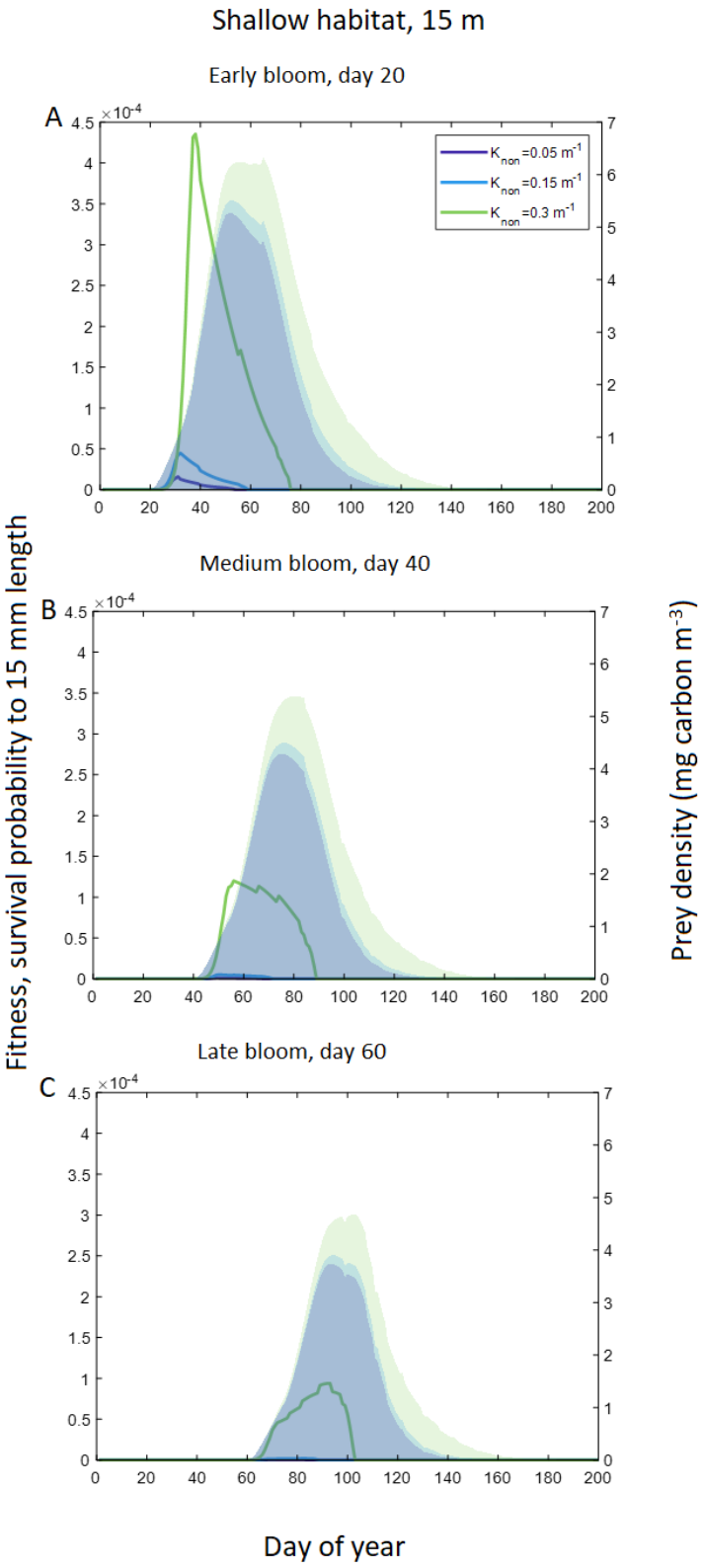

Figure A3: Simulation experiment at a shallower habitat (15 m depth). The panels represents scenarios where the phytoplankton bloom and Calanus production starts at day 20 (A), 40 (B), and 60 (C). Simulations were run for three different K_{non} values (0.05; 0.15; 0.3 m^{-1}). Shaded areas represents prey density, each colour corresponding to a different K_{non}. With low and medium light attenuation, fitness of hatching times were reduced compared to the normal scenario (fig. 5). An early and medium bloom with high light attenuation resulted in increased fitness compared to the normal scenarios, but the results show a decline in fitness related to a delayed bloom.

Appendix B – MATLAB code

```
% Bloom dynamics and calanus spawning
%*******************************************
% Calculates calanus mortality and spawning dynamics under different levels
of water clarity.
% Water clarity modulates mortality through parameter R, which is the
% detection range of a visual predator in a given chl a concentration. R-
values are
% calculated separately in Fortran and read from r-tables into MATLAB.
%*******************************************

close all;
clear all;

RunC6=1; %0=skip this part if C6 is allready estimated.

% general parameters
minDay=1;                % first day (DON'T CHANGE!)
maxDay=280;              % last day of simulation
daysinyear=365;
dayRes=24;               % time steps in a day (DON'T CHANGE!)

% parameters for Chla
chlaPeak = 100;          % time of chla peak in test distribution, day of
year
chlaMax = 5;             % ug chl a/m3,  Chla level at peak
chlaStD = 20;            % stD of bloom, days
chlaMin = 0;             % background chla level

%parameters for zooplankton
zooA = 0.004*0.001*0.75; % surface area of C6 calanus (m2),
length*width*0.75
zooCtr = 0.3;            % contrast
zooZ = 20;               % depth of zooplankton habitat, m
C6initAbun = 10;         % initial abundance of C6/m3
C6seedTime = 30;         % number of days C6 arrive to surface layer from
wake-up

aN1 = 595;               % a-parameter for egg to N1 development time in
Belehrádek temperature functions (Cambell, 2001)
aN5 = 3710;              % a-parameter for egg to N5
aC1 = 5267;              % a-parameter for egg to C1 development time..
p4 = 0.4;                % p4-parameter for estimating #eggs layed/female as
function of temperature (Fiksen and Carlotti, 1998)
p5 = 1.096;              % p5-parameter. (p5=1.096 in Fiksen and Carlotti);

NShape=0.5;              % generic shape of Nauplii, diam:length ratio
NCtr = 0.3;              % generic contrast
EggCtr = 0.3;

%mortalities (background/fixed)
C6mBack = 0.035;          % background C6 mortality, 0.04 day-1  Eiane et
al, 2002
eggM = 0.08;             % egg mortality per day,  Eiane et al, 2002
NM = 0.08;               % nauplii mortality d-1,  Eiane et al, 2002
C1M = 0.08;              % C1 mortality d-1, Eiane et al, 2002
```

```
%matrix length based on development time at low (4 deg) temperature.
C6ageMax = 100;             % not development time, but sufficiantly long
for all C6 to die.
EGGageMax = 4;              % sufficiantly long for all eggs to develop to
naupli (N)
N1ageMax = 17;              % sufficiantly long for all naupli (N) to
develop to C1(not modelled)
N5ageMax = 12;

% parameters for fish larvae
larvShape=0.2;                  % larval width : length ratio
larvCtr = 0.3;                  % contrast
larvDW2C = 0.4;                 % conversion from dry weight to carbon
(carbon makes up ca 40% of larval dry weight, Harris et al 1986)
larvC2DW = 1/larvDW2C;          % conversion from carbon to dry weight
(carbon makes up ca 40% of larval dry weight, Harris et al 1986)
larvInitWgt = 0.01 * larvC2DW;  % larval initial weight, mg carbon (0.03)
larvInitLen = 0.005;            % larval initial length, m (NOT USED)
larvAgeMax = 80;               % maximum age of larvae
larvSeedDayStart = 1;           % first day of larva modelling
larvSeedDayEnd = maxDay-larvAgeMax;     % last day
VisRtoSDPreyinBL=1;             % Detection distance in bodylengths (BL) of
small prey at satiating light and clear water (=1 BL for a 0.015 mm2 prey,
Fiksen & MacKenzie 2002)
larvKe = 1;             %
larvRelV = 1;                   % larval relative swimming speed (BL s-1)
larvVisFieldShape = 0.5;        % larval visuald field. 1 = 360 degrees
larvCP = 0.2;                   % larval prey capture probability (Fiksen &
MacKenzie 2002: 0.2)
larvHandTime = 0;               % larval prey handling time
larvAssimEff = 0.75;            % larval assimilation efficiency

% parameters for fish predator
fishLen = 0.3;          % length of fish, meters
fishKe = 1;             % fish light satiation, umol p m-2 s-1
fishV = 0.3;            % fish swimming speed, m s-1
fishVisFieldShape = 0.5;% fish eye angle, degrees
fishHandTime =2;        % handling time for fish predator, sec
fishAbun = 1E-4;        % density of fish predators, #/m3
fishEMzoo=50000;        % eye sensitivity when feeding on zooplankton

% parameters for surface light
cloudCover=0.5;         % cloud cover
pi2=8.*atan(1.);
dLat=68;%68;            % pick appropriate latitude
rLat=dLat*(pi2/360);    %latitude in radians;

% parameters for light at depth down to zZoo
kNon= [0.05 0.15 0.3];        % non chlorophyll light attenuation, m-1

%% SET ENVIRONMENT
% load temperature from 3D matrix:
load TempMat.mat %loading temperature data 3D-matrix MatT: [depth(0:100),
lat(58:0.1:71), day (1:365)].
latRes=58:0.1:71;
f=latRes==dLat;
Temp=squeeze(MatT(:,f,:)); %Temp at 68degN

% create idal seasonal temperature by smoothing. Used to estimate
development time (Behlradek)
```

```
f=fit([1:daysinyear]',mean(Temp(1:zooZ,:))','poly5');
Temp=f(1:daysinyear)*0+4.7; % set new idealized seasonal temperature

%Conceptual chl a bloom
chlaSurf=chlaMin+chlaStD*(chlaMax-chlaMin)*2.5*pdf('normal', minDay:maxDay,
chlaPeak,chlaStD); %normal distribition function
mean(chlaSurf)      %should be ~1 (Vikebø et al 2012)
chlaOnset=find(chlaSurf>0.05, 1); %day of bloom onset

% chlorophyl concentration from surface to zZoo (depth of zooplankton)
Chla(1:zooZ, minDay:maxDay)=repmat(chlaSurf, zooZ,1); % currently
chlorophyll concentation is same in depth as surface


%% C6 ZOOPLANTON MODEL

C6WakeUp=chlaOnset; % decide if wake up day for C6 should be (in)dependent
of spring bloom
% C6WakeUp=40;

if RunC6==1 %  run C6 loop below
   for k=1:length(kNon) %loop over different k-non values

       %C6 model
       C6=zeros(maxDay,C6ageMax); % empty matrix for C6

        for julDay=minDay:maxDay-1              % loop over days
            if julDay > C6WakeUp && julDay<C6WakeUp+C6seedTime
                C6(julDay,1)=C6initAbun;        %add C6 to age 1
            else
            end
            for age=1:C6ageMax-1                % loop over C6 ages
                C6mRateFishSum=0;               % reset daily C6 mortality
rate from fish to zero
                C6Abun=C6(julDay,age);



                for t=1:dayRes                  %loop over hours
                    Eb = zeros(zooZ+1,1);         % empty matrix of ambient
light at depth  Replaced every hour
                    % calculate surface light and light at depth
                    Eb(1) = qsw0(cloudCover,rLat,julDay,t) * 4.6; % surface
light in umol p m-2 s-1, calls SUBROUTINE QSW0()

                    for z=2:zooZ+1      %light at depth. Note that 1st row
in Eb is surface (calculated outside the z-loop)
                        DiffAtt = kNon(k) + Chla(z-1,julDay)*(0.0506*exp(-
0.606*Chla(z-1,julDay))+0.0285)+(0.068*exp((-0.014)*(550-550)));  % Coastal
type 2, equations 13 and 15 in Wozniak et al 2003
                        BeamAtt = (kNon(k)*2) + (0.39*(Chla(z-
1,julDay)^0.57))*(1.563 - 0.001149*550);
% equations 3.47 and 3.48 in Mobley (Voss 1992)
                        Eb(z) = Eb(z-1)*exp(-DiffAtt);
                    end
                    if Eb(zooZ+1)>0 % if there is light (Eb>0)

r=getr(BeamAtt,zooCtr,zooA,fishEMzoo,fishKe,Eb(zooZ+1)); % find visual
range (m) of a fish at depth zooZ,  call SUBROUTINE GETR()
                    else
```

```
                        r=0;
                    end
                    %calculate hourly mortality from visual feeders (fish)
at zooZ (a fixed depth):
                    if C6Abun>0
%if C6Abun is >0, calculate mortality from fish ....
                        fishClear = fishVisFieldShape*pi*(r^2)*fishV;
%find the volume cleared by a fish m3 s-1
                        fishIng =fishClear*C6Abun/(1 +
fishClear*fishHandTime*C6Abun);  % fish ingestion rate,calanus per fish per
second (handling time limited)
                        C6mRateFish = fishIng*fishAbun/C6Abun;
% calanus mortality rate, s-1
                    else
                        C6mRateFish=0;
% *** ... otherwise set mortality from fish to zero
                    end
                    C6mRateFishSum=C6mRateFishSum + C6mRateFish*3600;
% sum the mortality rates per hour (3600 sec)
                end % hour
                C6mFish = 1-exp(-C6mRateFishSum);
% C6 mortality from fish, probability of dying per day
                %C6m=max(C6mFish, 1-exp(-C6mBack));
% C6 mortality overall. Cannot be lower than daily background mortality
(C6mBack)
                C6m=1-exp(-C6mBack -C6mRateFishSum);
% C6 mortality overall. Cannot be lower than daily background mortality
(C6mBack)
                C6(julDay+1,age+1)=C6(julDay,age)- C6(julDay,age)*C6m;
% remove eaten C6 from population (mortality) and tranfer survivors to the
next day and age

            end % age

        end % julian days
    C6_All(:,:,k)=C6;
    end %kNon values

    save C6_AllK.mat C6_All

else % if not running C6 loop
    load C6_AllK.mat; %read C6 from file
end

% sum all C6 age classes
C6sum=[];
for k=1:length(kNon)
    C6sum(:,k)=nansum(C6_All(:,:,k),2);
end

%% EGG AND NAUPLII MODEL
% generate empty matrices
EGG_All=zeros(maxDay, EGGageMax, length(kNon));
N1_All=  zeros(maxDay, N1ageMax, length(kNon));
N5_All=  zeros(maxDay, N5ageMax, length(kNon));

for k=1:length(kNon) % loop over different R-values
    C6=C6_All(:,:,k); % extract C6 abundances generated in the C6 model
    EGG= zeros(maxDay, EGGageMax);
    N1=   zeros(maxDay, N1ageMax);
```

```
    N5=   zeros(maxDay, N5ageMax);
    for julDay=minDay:maxDay-1 % loop over all days

        time2N1= int32(aN1*(Temp(julDay) + 9.11)^-2.05);            %
development time from egg to N1 in Belehrádek temperature functions
(Cambell, 2001)
        time2N5 = int32(aN5*(Temp(julDay) + 9.11)^-2.05) - time2N1;
        time2C1= int32(aC1*(Temp(julDay) + 9.11)^-2.05) - time2N5;  %
development time from N1 to C1

        eggNo = 12*p4*p5^Temp(julDay);                              %
number of eggs/female/day as function of Temp (Fiksen and Carlotti, 1998)

        % egg loop
        EGG(julDay,1)=sum(C6(julDay,:))*eggNo;
        for age=1:time2N1
           EGG(julDay+1, age+1)= EGG(julDay,age) - EGG(julDay, age)*eggM;
%remove daily agg mortality (eggN)
        end

        % Nauplii 1-4 loop
        N1(julDay,1)=EGG(julDay, time2N1);
        for age=1:time2N5
            N1(julDay+1,age+1)=N1(julDay,age) - N1(julDay,age)*NM; % remove
daily naupli mortality (NM)
        end

        N5(julDay,1)=N1(julDay, time2N5);
        for age=1:time2C1
            N5(julDay+1,age+1)=N5(julDay,age) - N5(julDay,age)*NM; % remove
daily naupli mortality (NM)
        end

    end % julDay
    % Store for all kNon-values
    EGG_All(:,:,k)=EGG;
    N1_All(:,:,k)=N1;
    N5_All(:,:,k)=N5;
end % kNon loop

%Sum all age groups
for k=1:length(kNon)
    EGGsum(:,k)=nansum(EGG_All(:,:,k),2);
    N1sum(:,k)=nansum(N1_All(:,:,k),2);
    N5sum(:,k)=nansum(N5_All(:,:,k),2);
end

%% LARVAL FISH MODEL
WGT_All=[]; SURV_All=[]; LEN_All=[]; PREYMASS_All=[];

Check=[];Check2=[];
for k=1:length(kNon) %loop over different k-non values

    WGT = zeros(maxDay, larvAgeMax+1);
% initial matrix for weight, mg carbon
    LEN = zeros(maxDay, larvAgeMax+1);
% initial matrix for length, m
```

```
    SURV = zeros(maxDay, larvAgeMax+1);
% initial matrix for survival. Per Jan 31, this only includes visual
predators.
    PREYMASS = zeros(maxDay, larvAgeMax+1);

    WGT(larvSeedDayStart:larvSeedDayEnd,1) = larvInitWgt;
% initial weight, Carbon, at seed day
    LEN(larvSeedDayStart:larvSeedDayEnd, 1)=1E-
3*exp((log(larvInitWgt*larvC2DW)+9.2)/3.9);      % initial length in m
(from dry weight), from Otterlei & al 1999
    SURV(larvSeedDayStart:larvSeedDayEnd,1)=1;

    for seedDay=larvSeedDayStart:larvSeedDayEnd
% follow larva from different seed days

        for julDay=seedDay:seedDay + larvAgeMax
% loop over days of the
            age=julDay-seedDay +1;
% find age. Add +1, so age starts at age 1 (day)

            LmRateFishSum = 0;
% reset daily mortality estimate
            larvPreyMassEncSum = 0;
% reset sum of larval prey mass encounter
            Eb = zeros(zooZ+1,1);
% empty vector of ambient light at depth (zooZ+1 = 15 m) and t (hour).
Replaced every new day

            preyAbun=EGGsum(julDay,k) + N1sum(julDay,k) + N5sum(julDay,k);
% Sum abundance of all available prey (# m-3) that day

            % estimates of temperature dependent egg and nauplii sizes
(Area, m2) (from Table 2 in Campbell, 2001)
            EggA = pi*((-0.405*Temp(julDay)+147)*1E-6/2)^2;
% surface area of an egg (m2) assuming circular shape
            N1L = (-0.250*Temp(julDay)+ 310)*1E-6;
% length (m) of Naupli stage 1-4 (Table 2 in Campbell 2001)
            N1A = pi*(N1L*NShape)*N1L*0.75;
% Area (m2) of Naupli stage 1-4
            N5L = (-3.75*Temp(julDay) + 607)*1E-6;
% length (m) of Nauplii stage 5-6 (Table 2 in Campbell 2001)
            N5A = pi*(N5L*NShape)*N5L*0.75;
% Area (m2) of Nauplii stage 5-6

            preyA = (EGGsum(julDay,k)*EggA + N1sum(julDay,k)*N1A +
N5sum(julDay,k)*N5A)/ preyAbun;      % weighted mean prey Area (m2) based
on the abundance of eggs, N1-4 (N1) and N5-6 (N5)
            preyCtr = (EGGsum(julDay,k)*EggCtr + N1sum(julDay,k)*NCtr +
N5sum(julDay,k)*NCtr)/ preyAbun;% Weighted mean prey contrast

            % estimates of temperature dependent egg and nauplii carbon
content (mg) (from Table 2 in Campbell, 2001)
            EggC = (-0.00255 * Temp(julDay) + 0.216) * 1E-3 ;
% egg carbon weight, mg
            N1C = (9.46E-4 * Temp(julDay) + 0.226) * 1E-3;
% N1-4 carbon weight, mg
            N5C = (-0.0117 * Temp(julDay) + 1.825) * 1E-3;
% N5-6 carbon weight, mg
```

```
            preyMass = (EGGsum(julDay,k)*EggC + N1sum(julDay,k)*N1C +
N5sum(julDay,k)*N5C)/ preyAbun;% weighted mean prey carbon weight, mg

            %loop over hours
            for t=1:dayRes

                % calculate surface light and light at depth
                Eb(1) = qsw0(cloudCover,rLat,julDay,t) * 4.6;
% surface light in umol p m-2 s-1
                for z=2:zooZ+1
% light at depth. Note that 1st row in Eb is surface (calculated outside
the z-loop)
                    DiffAtt = kNon(k) + Chla(z-1,julDay)*(0.0506*exp(-
0.606*Chla(z-1,julDay))+0.0285)+(0.068*exp((-0.014)*(550-550)));  % Coastal
type 2, equations 13 and 15 in Wozniak et al 2003
                    BeamAtt = (kNon(k)*2) + (0.39*(Chla(z-
1,julDay)^0.57))*(1.563 - 0.001149*550);
% equations 3.47 and 3.48 in Mobley (Voss 1992)
                    Eb(z) = Eb(z-1)*exp(-DiffAtt);
                end
                % find larva's visual range when feeding on zoopl. prey
                if Eb(zooZ+1)>0 && preyAbun>0
% if there is light (Eb>0) and prey is present.


larvEM=((LEN(julDay,age)*VisRtoSDPreyinBL)^2.)/(preyCtr*(0.1*0.2*0.75*1E-
6)); % larval eye sensitivty (EM) depend on bodylength and prey size
                    r=getr(BeamAtt,preyCtr,preyA,larvEM,larvKe,Eb(zooZ+1));
% find visual range (m) of a fish at depth zooZ,  call SUBROUTINE
GETR(r,c,C0,Ap,Vc,Ke,Eb,IER) Aksnes & Utne 1997

                    % Larval feeding
                    larvV=LEN(julDay, age)*larvRelV;
% larval swimming speed, m s-1
                    larvClear = larvVisFieldShape*pi*(r^2)*larvV;
% larval clearance rate, m3 s-1
                    larvPreyMassEnc =
(larvCP*larvClear*preyAbun*preyMass)/(1+larvClear*preyAbun*larvHandTime); %
mg Carbon encountered per second
                else
                   larvPreyMassEnc=0;
                end
                larvPreyMassEncSum = larvPreyMassEncSum +
larvPreyMassEnc*3600;     % sum prey mass encounter carbon per hour (3600
s) through a day (24 H)

                % Find predator's visual range
                if Eb(zooZ+1)>0
% if there is light (Eb>0)
                    larvW = larvShape*LEN(julDay, age);
% larval width,m
                    larvA = larvW*LEN(julDay, age)*0.75;
% larval area, m2
                    fishEM=((fishLen*VisRtoSDPreyinBL)^2)/(larvCtr*larvA);
% eye sensitivity (previously em=50000)
                    r=getr(BeamAtt,larvCtr,larvA,fishEM,fishKe,Eb(zooZ+1));
% find visual range (m) of a fish at depth zooZ,  call SUBROUTINE
GETR(r,c,C0,Ap,Vc,Ke,Eb,IER)
                else
                    r=0;
```

```
                end
                %calculate hourly mortality from visual feeders (fish) at
zooZ (a fixed depth):
                fishClear = fishVisFieldShape*pi*(r^2)*fishV;
% find the volume cleared by a single fish m3 s-1
                fishEncRate = fishClear*fishAbun;
% lethal encounters with fish predator (not handling time limited), s-1
                LmRateFishSum=LmRateFishSum + fishEncRate*3600;
% sum the mortality rates per hour (3600 sec) through a day (24 H)

            end % hour

            % calculate daily growth
            wgt=WGT(julDay,age)*larvC2DW;
% get larval weight (mg Carbon) and convert to mg DW
            if wgt>0.03
% check if within range of SGR equation
                temp=Temp(julDay);
% get temperaure that day
                R = 2.38E-7 * exp(0.088*temp);
% Respiration from Finn & al. (2002), g dWeight/sec
                larvResp = (wgt^0.9)*R*86400*larvDW2C;
% respiration in carbon/day

                SGR = 1.2 + 1.8*temp - 0.078*temp*(log(wgt)) -
0.0946*temp*(log(wgt))^2 + 0.0105*temp*(log(wgt))^3; % max temp dep growth,
mg DW day-1 (Folkvord 2005)
                larvSGR=log((SGR/100) + 1);%
% max daily growth rate (weight/weight /day) .

                larvDelta=(larvResp +
larvSGR*WGT(julDay,age))/larvAssimEff;    % food needed to sustain max
growth
                if larvDelta<larvPreyMassEncSum
% if daily food intake kan sustain max growth (SGR)...
                    larvGrowth = WGT(julDay,age)*larvSGR;
% estimat max absolute growth in mg Carbon
                else
% if not..
                    larvGrowth = larvPreyMassEncSum*larvAssimEff -
larvResp;    % growth  = assimilated food - respiration, mg Carbon
                end

                larvMBack=(2.2*1E-4 * (wgt*1E-3)^-0.85) * 0.5;
% background mortality, day-1 (NOTE: we multiply by 0.5 to account for
visual pred)

                WGT(julDay+1,age+1)=WGT(julDay,age) + larvGrowth;
% add growth to weight, mg C
                %SURV(julDay,age) = min(exp(-LmRateFishSum), exp(-
larvMBack));   % survival probability
                SURV(julDay+1,age+1) = exp(-LmRateFishSum-(larvMBack));   %
survival probability
                LEN(julDay+1,age+1) = 1E-
3*exp((log(WGT(julDay+1,age+1)*larvC2DW)+9.2)/3.9); % estimate length, m

            else % if the larva is smaller than 0.03 mg

                WGT(julDay+1,age+1)=0; % set weight to zero, mg C
                SURV(julDay+1,age+1) = 0;
```

```
                LEN(julDay+1,age+1) = 0 ; % set length, m to zero
            end % check on minimum weight requirement

            PREYMASS(julDay+1,age+1)=preyMass; %store prey mass


        end %julian day
    end % seed days

    % store results for different kNon-values
    WGT_All(:,:,k)=WGT;
    SURV_All(:,:,k)=SURV;
    LEN_All(:,:,k)=LEN;
    PREYMASS_All(:,:,k)=PREYMASS;
end %kNon values
```